Thermochimica Acta, 34 (1979) 19—28

THERMOANALYTICAL STUDY ON THE CHLORINATION OF HYDRATED ALUMINAS AND TRANSITION ALUMINAS

T. TSUCHIDA, T. ISHII, R. FURUICHI and H. HAGA

Department of Applied Chemistry, Faculty of Engineering, Hokkaido University, Sapporo 060 (Japan)

(Received 4 January 1979)

ABSTRACT

The chlorination processes of four hydrated aluminas (bayerite, gibbsite, pseudo-boehmite, boehmite) and four transition aluminas (η-, γ-, δ-, θ-Al_2O_3) were studied in the presence of active carbon by means of a gas-flow DTA apparatus. In the case of hydrated alumina systems three exothermic peaks appeared at about 230, 460 and 500°C or above, which corresponded to the formation of hydrogen chloride, white needle-like crystals and the chlorination of hydrated aluminas, respectively. On the other hand, in transition alumina systems, only one exothermic peak due to the chlorination of transition alumina appeared at 580—670°C. The relationship between the chlorination behavior and structure of transition aluminas was discussed.

INTRODUCTION

Chloride metallurgy has been one of the most important techniques in process metallurgy. Recently, this technique has been noted not only from the standpoint of thermodynamics but also from that of kinetics. The authors have previously designed a simple gas-flow DTA apparatus which can be used in a corrosive chlorine atmosphere. By using it, thermoanalytical investigations have been done on the chlorination behaviors of various Mg-containing ores [1], viz. magnesia, olivine, prototensatite and talc, and Al-containing ores [2] such as bauxite. The relationship between chlorination behaviors and structures and compositions of the ores has been also discussed.

In this paper, the chlorination behavior and reactivity of hydrated aluminas which are the principal constituent of bauxite, and transition aluminas obtained by thermal decomposition of hydrated aluminas have been studied in detail by means of this gas-flow DTA apparatus.

EXPERIMENTAL

Materials

Hydrated aluminas and transition aluminas used in chlorination experiments were prepared as follows.

Gibbsite, α-$Al_2O_3 \cdot 3\,H_2O$, was prepared by the hydrolysis of a 10 wt.% solution of sodium aluminate at 50°C for 72 h. The precipitate was filtered, washed with hot distilled water (ca. 60—70°C) until the pH of the filtrate reached 5.4, and then dried at 130°C for 15 h. X-Ray diffraction of the product revealed the presence of well-crystallized gibbsite with traces of boehmite and bayerite.

Bayerite, β-$Al_2O_3 \cdot 3\,H_2O$, was obtained from a gel precipitated at 8—10°C by adding a 10 wt.% solution of aluminum nitrate to 4 M ammonium hydroxide at a dropping speed of 3—6 ml min^{-1} and a constant speed of stirring. After being left to age in the mother liquor (pH = 10.8—11.0) at 13°C for 24 h, the gel was filtered, washed and then dried in a vacuum drying oven at 50—60°C for 36 h. Well-crystallized bayerite was confirmed by X-ray diffraction.

Pseudoboehmite, $Al_2O_3 \cdot n\,H_2O$ ($1.3 < n < 1.8$) [3], sometimes also called gelatinous boehmite, was prepared at room temperature by adding a 10 wt.% solution of aluminum nitrate to 4 M ammonium hydroxide to pH = 8.7 at a dropping speed of ca. 13 ml min^{-1} with stirring. The precipitate was filtered immediately without ageing, washed and dried at 120°C for 8 h. The n value of the product was estimated from gravimetric analysis to be 1.6 moles.

Boehmite, α-$Al_2O_3 \cdot H_2O$, was hydrothermally synthesized from pseudoboehmite in an autoclave under conditions of vapor pressure 88 kg cm^{-2}, 280°C and 5 h. The precipitate was dried at 125°C for 11 h. Well-crystallized boehmite was confirmed by X-ray diffraction.

Transition aluminas were prepared by calcination of various hydrated aluminas described above in a lateral furnace and in air at 600 and 900°C for 3 h, respectively (see Table 2). All reagents used were of GR grade, except for sodium aluminate which was of EP grade, and were supplied from Kanto Chemical Co. Inc..

Chlorination

Hydrated aluminas and transition aluminas were sieved to obtain −300 mesh fractions and subsequently mixed with active carbon (C) in a weight ratio of sample/C = 2 and in a V-type mixer for 1 h, respectively. A mixture of about 500 mg was used in a DTA experiment. The gas-flow DTA apparatus used, as already described [1], consists of two quartz tubes (i.d. = 10 mm, length = 550 mm) placed vertically in a furnace, one used as a reference holder and the other as a sample holder. The chlorination experiments were carried out at a Cl_2 flow rate of 30 ml min^{-1} and at a heating rate of 5°C min^{-1}. During the experiments, chlorine gas flowed through the reference holder into the sample holder. In order to analyze the samples in the course of DTA runs, the samples heated to various temperatures were taken out of the furnace and quenched to room temperature after the chlorine in the holders was purged with nitrogen (30 ml min^{-1}) for 1 h. Samples were then subjected to X-ray diffraction and chemical analysis.

The fractional conversion, α, of chlorinated samples was calculated from the difference between the amounts of Al^{3+} in the samples before and after the reaction, as described below. After the chlorination experiments, the

sample in its sample holder was washed with distilled water in order to remove chlorides and then residual alumina was dissolved in a solution of mixed acid [1] (H_2O : H_2SO_4 : HNO_3 : HCl = 9 : 3 : 2 : 6 in volume ratio) plus H_2SO_4 by boiling for 1 h. The solution was filtered, and the amount of Al^{3+} in the filtrate was determined by backtitration using XO indicator and standard lead nitrate solution [5]. The accuracy of α was estimated to be within ±3%.

RESULTS AND DISCUSSION

Chlorination of hydrated aluminas

Figure 1 shows DTA curves of the hydrated alumina—active carbon (C) systems in chlorine and nitrogen. Curves (a)—(c) show the DTA curves for the bayerite system, curves (d)—(f) for the gibbsite system, curves (g) and (h) for the pseudoboehmite system, and curves (i) and (j) for the boehmite system, respectively. X-Ray diffraction results of samples, quenched from the various temperatures shown by the arrows on DTA curves in nitrogen, were also shown in the figure. In addition, Fig. 2 shows the fractional conversions (α) of samples chlorinated up to the temperatures shown by the arrows in Fig. 1. Curve (c) in Fig. 1 shows the DTA curve of the bayerite—C system in N_2. A large endothermic peak corresponding to the dehydration of bayerite appeared at about 300°C. X-Ray diffraction patterns of the sample heated to 330°C showed the formation of η-Al_2O_3. Curve (a) shows the DTA curve of the bayerite—C system in Cl_2. Three exothermic peaks appeared at 230, 460 and 500°C, respectively. The exothermic reaction with its peak at 500°C seems to be due to the chlorination of bayerite since the fractional conversion, as shown in Fig. 2, increased steeply at temperatures above 480°C. In the vicinity of the onset temperature of this peak, white and yellow products began to stick to the top of sample holder. X-Ray diffraction of the products obtained at 600°C revealed the presence of $AlCl_3 \cdot 6\,H_2O$ alone, which could have been formed by hydration of the chlorination product such as $AlCl_3$ by atmospheric moisture. The reaction with its peak at 460°C will be described later. The temperature range between 200 and 300°C, where a complex exothermic peak appeared in curve (a), corresponds to that of the dehydration of bayerite shown in curve (c). Therefore, it is presumed that this complex exotherm is due to the superposition of some exothermic reaction on the endotherm of dehydration of bayerite. This exothermic reaction is considered to be the formation of hydrogen chloride by the reaction of water vapor with chlorine in the presence of active carbon, i.e.,

$$Cl_2(g) + H_2O(g) + C(s) \rightarrow 2\,HCl(g) + CO(g) \qquad (1)$$

The calculated enthalpy and free energy of this reaction were $\Delta H = -12$ kcal mole^{-1} and $\Delta G = -26 \sim -45$ kcal mole^{-1} in the temperature range of 100—600°C. Curve (b) shows the DTA curve of the dehydrated bayerite—C system in Cl_2, which was obtained by preheating the bayerite—C system up to

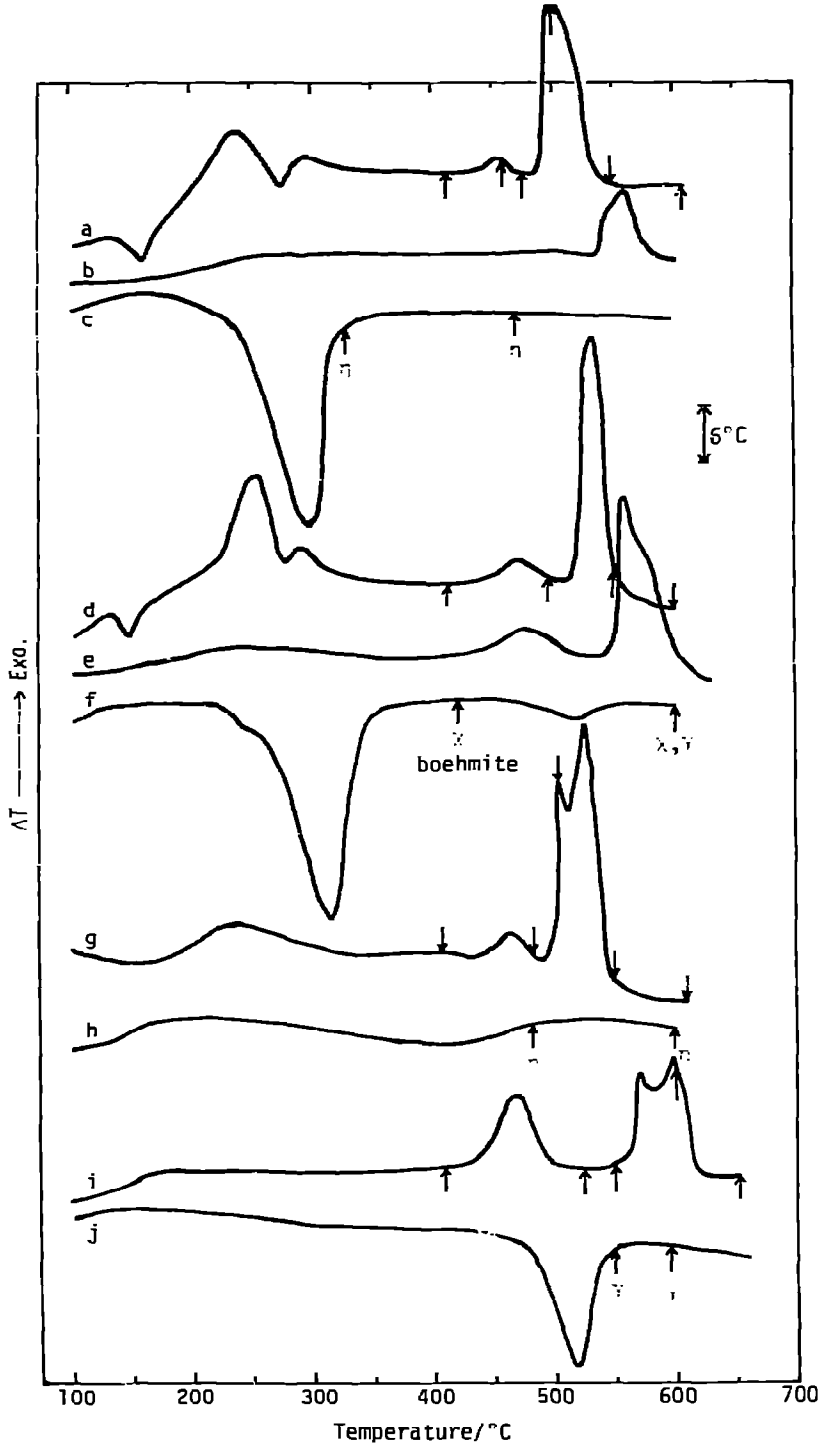

Fig. 1. DTA curves of hydrated alumina-active carbon (C) systems (wt. ratio 2 : 1) in chlorine (Cl_2) and nitrogen (N_2). Flow rate of Cl_2 and N_2, 30 ml min^{-1}; heating rate, 5°C min^{-1}; total weight of sample, 475—525 mg. (a), bayerite—C—Cl_2; (b), dehydrated bayerite*—C—Cl_2; (c), bayerite—C—N_2; (d), gibbsite—C—Cl_2; (e), dehydrated gibbsite*—C—Cl_2; (f), gibbsite—C—N_2; (g), pseudoboehmite—C—Cl_2; (h), pseudoboehmite—C—N_2; (i), boehmite—C—Cl_2; (j), boehmite—C—N_2.

* These were obtained by heating systems (c) and (f) to 390°C, respectively.

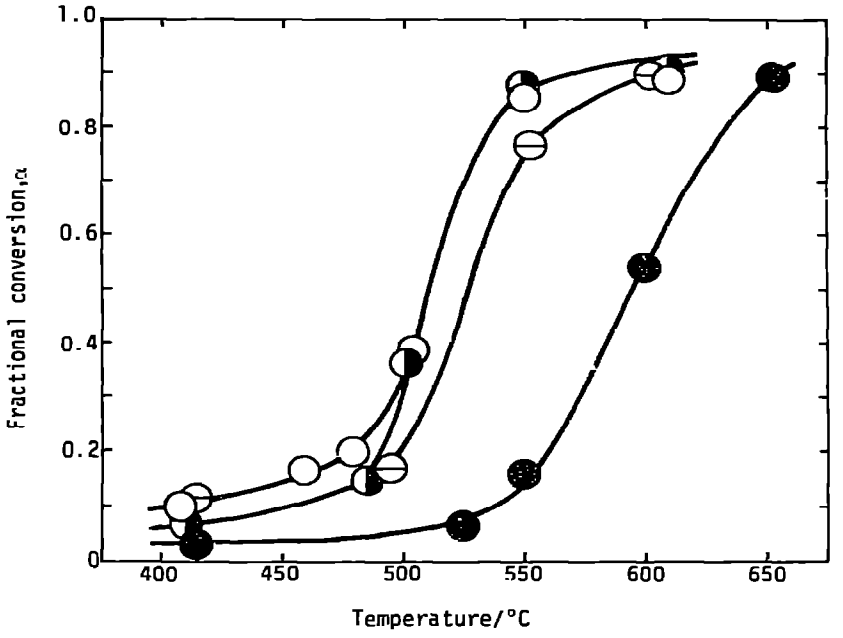

Fig. 2. Fractional conversion (α) of samples chlorinated vs. temperatures shown by the arrows on DTA curves in Cl_2 in Fig. 1. ○, bayerite system [curve (a) in Fig. 1]; ◑, pseudo-boehmite system [curve (g)]; ⊖, gibbsite system [curve (d)]; ●, boehmite system [curve (i)].

390°C in N_2. The exothermic peaks at 200—300°C and 460°C seen in curve (a) disappeared and only one exothermic peak corresponding to the chlorination of dehydrated bayerite (probably η-Al_2O_3) appeared at about 560°C, which is a higher temperature by ca. 60°C than that of the chlorination of bayerite shown in curve (a). From these facts, it is suggested that the water vapor resulting from the dehydration of bayerite participates in the exothermic reaction between 200 and 300°C. No chlorination reaction occurred in the system consisting of bayerite alone without active carbon at temperatures below 600°C and the shape of the DTA curve was nearly the same as that of curve (c).

In the case of the gibbsite—C system shown in curves (d)—(f), the shape and position of the DTA peaks are observed to be similar to those in the bayerite—C system. The X-ray diffraction pattern of a sample heated to 220°C in curve (f) showed that the ratio of X-ray intensities of boehmite to gibbsite was twice that of the starting materials. The sample heated further to 420°C consisted of χ-Al_2O_3 and boehmite which decomposed endothermically to γ-Al_2O_3 at about 520°C. On the basis of these results, it is found that in flowing N_2 [curve (f)] a small endothermic peak at 220—260°C corresponds to a partial decomposition of gibbsite to boehmite and a large endothermic peak at about 315°C corresponds to the decomposition of gibbsite to χ-Al_2O_3. Curve (d) in flowing Cl_2 is very similar to curve (a) in the shape and position of its DTA peak except that the last large exothermic peak due to the chlorination of hydrated alumina in curve (d) is shifted to a higher

temperature by about 30°C than that in curve (a). Curve (e) shows the DTA curve of the dehydrated gibbsite—C system in Cl_2, which was obtained by preheating the gibbsite—C system to 390°C in N_2. An exothermic peak between 200—300°C shown in curve (d) disappeared in this system and a large exothermic peak due to the chlorination of dehydrated gibbsite was also shifted to a higher temperature by about 30°C than that for gibbsite shown in curve (d). On the other hand, a small exothermic peak at around 480°C did not disappear. This seems to be due to the presence of undecomposed boehmite in the sample heated to 390°C [see curve (i)].

Curves (g) and (h) show the DTA curves of the pseudoboehmite—C system in Cl_2 and N_2, respectively. In the case of flowing N_2 [curve (h)], the pseudoboehmite was dehydrated over a wide range from 250 to 500°C and transformed to η-Al_2O_3 at 480°C. In flowing Cl_2 [curve (g)], the exothermic peaks at 200—300°C and 500—550°C correspond to the reaction expressed by eqn. (1) and to the chlorination of pseudoboehmite, respectively.

Curves (i) and (j) show the DTA curves of the boehmite—C system in Cl_2 and N_2. In the case of flowing N_2 [curve (j)], the endothermic peak due to the dehydration of boehmite appeared at about 520°C and γ-Al_2O_3 was formed at 550°C. In flowing Cl_2 [curve (i)], the exothermic peaks corresponding to chlorination of boehmite appeared at about 470°C and 560—620°C. The exothermic peak at 470°C is the largest among all the hydrated alumina systems.

From the results shown in Figs. 1 and 2, the chlorination behavior of various hydrated aluminas is summarized as follows.

Firstly, the exothermic peak appears at around the onset temperature of dehydration of each hydrated alumina. This seems to correspond to the reaction expressed by eqn. (1).

Secondly, the small exothermic peak appears at 450—470°C in all systems. The onset temperatures of the peak are also nearly constant, i.e. 430 – 440°C, in spite of the differing kinds of hydrated aluminas. Moreover, as shown in Fig. 1, curve (b), this small exothermic peak was not observed when the sample had been previously dehydrated. This suggests that water vapor or hydrogen chloride resulting from the reaction expressed by eqn. (1) participates in this exothermic reaction. In fact, a small amount of white needle-like crystals were observed to grow on the upper part of the thermocouple sheath, put into a sample holder, towards the final temperatures of the exothermic peaks: 483°C for bayerite system in curve (a); 482°C for gibbsite system in curve (d); 478°C for pseudoboehmite system in curve (g); 519°C for boehmite system in curve (i). The amount of crystals obtained increased in the order bayerite, pseudoboehmite, gibbsite and boehmite systems. Table 1 shows the X-ray diffraction data of the needle-like crystals obtained in the boehmite system. In all hydrated alumina systems, the X-ray diffraction lines of the crystal obtained had the same *d*-spacings though they differed in intensity. The data shown in Table 1 were compared with the diffraction lines of aluminum chloride, aluminum oxide chloride and aluminum chloride hydroxide hydrates from ASTM cards. However, no material which corresponded to the data in Table 1 was found. Since the needle-like crystals obtained in all hydrated alumina systems have the same diffraction lines, it

TABLE 1

Characteristic d-spacings of needle-like crystals obtained by heating the boehmite system up to 519°C in Fig. 1, curve (i)

d (Å)	I	d (Å)	I
7.43	25	2.66	6
7.19	100	2.62	28
6.96	35	2.39	11
4.13	4	1.96	6
4.02	8	1.85	2
3.70	12	1.80	17
3.59	67	1.74	5
3.48	15	1.59	3
2.81	5	1.54	8
2.77	30	1.39	5
2.74	12		

seems reasonable to assume that the crystal is not a mixture but a single phase. Chemical analysis confirmed the presence of Al^{3+} and Cl^- ions as the constituents of the crystal. From the above results, it is considered that the white crystal could be a kind of chloride formed by chlorination. Details of its structure are under investigation. Furthermore, as found in Fig. 1, the boehmite—C system [curve (i)] gives the largest exothermic peak corresponding to the formation of the needle-like crystals. This seems to be attributable to the simultaneous occurrence of the formation of needle-like crystals and an exothermic reaction expressed by eqn. (1). The latter reaction supplies water vapor or hydrogen chloride in enough quantity to form the needle-like crystals. This may be supported by the fact that the onset temperature of an exothermic peak due to the needle-like crystal formation agrees approximately with that of the dehydration of boehmite.

Thirdly, in all hydrated alumina systems the large exothermic peak appears at temperatures above 500°C, which corresponds to the formation reaction of aluminum chloride (identified as the hexahydrate because of its reaction with atmospheric moisture). This is also supported from the results in Fig. 2 which show a marked increase in fractional conversion at temperatures above 500°C. When the onset temperature of the exothermic peak is taken as a measure of the reactivity of hydrated aluminas for the chlorination reaction, the reactivity decreases in the following order: bayerite (onset temperature 487°C); pseudoboehmite (490°C); gibbsite (513°C); boehmite (555°C). The results for fractional conversion in Fig. 2 also show the same tendency to adopt this order of reactivity. As shown in Fig. 1, all exothermic peaks due to chlorination appear at temperatures above the dehydration temperatures of hydrated aluminas. It is, therefore, expected that the difference in reactivity is related to structures and textures of transition aluminas formed by the dehydration of hydrated aluminas. Thus the chlorination reaction of transition aluminas themselves was next investigated.

Chlorination of transition aluminas

Table 2 shows the preparation conditions, phases identified by X-ray diffraction and specific surface areas of various transition aluminas, which were obtained by isothermal calcination of hydrated aluminas. It also indicates that the courses of transition are bayerite → η → θ and boehmite → γ → δ, which agree with those reported previously [6]. On the other hand, η- and θ-Al_2O_3 were formed in the course of the thermal decomposition of gibbsite. The transition course of gibbsite → η → θ differs from that shown in Fig. 1, curve (f), i.e. gibbsite → χ → κ (called χ-series). The difference in the transition process seems to be ascribed to the heating rate of the sample, that is, when the sample was placed in a furnace kept at 600 or 900°C, it was rapidly heated, whereas it was heated slowly at a rate of 5°C min^{-1} in the case of Fig. 1, curve (f). Similar results have also been reported by Tertian and Papée [7]. In addition, as shown in Table 2, a small amount of γ- and δ-Al_2O_3 is formed in the course of the decomposition of gibbsite. It is considered that these transition aluminas were obtained by the thermal decomposition of boehmite which was present in starting materials and was formed in gibbsite under intragranular hydrothermal conditions [3].

Figure 3 shows the DTA curves of chlorination of the transition aluminas shown in Table 2. Only one exothermic peak corresponding to chlorination of the transition aluminas appeared in the respective systems at a temperature higher by 80—100°C than that in hydrated alumina systems. The fractional conversion (α) of samples chlorinated up to the final temperature of the DTA experiments exceeded 90% in all systems. The chlorination product was aluminum chloride hexahydrate alone and needle-like crystals did not form. The onset temperatures of exothermic peaks are T_i = 564, 571, 571, 586, 633 and 650°C for curves (a)—(f), respectively. These temperatures were reproducible within ±4°C on repeated runs. Taking these onset temperatures as a measure of the reactivity for chlorination of transition aluminas as well as hydrated aluminas, it is found that the reactivity of η- and θ-Al_2O_3 shown in curves (a)—(d) is generally higher than that of γ- and δ-

TABLE 2

Transition aluminas prepared by the calcination of various hydrated aluminas

Specimen no.	Starting material	Calcination conditions		Transition aluminas identified	Specific surface area (m^2/g)
		Temp. (°C)	Time (h)		
a	Bayerite	600	3	η	180
b	Bayerite	900	3	θ	95
c	Gibbsite	600	3	$\eta > \gamma$	158
d	Gibbsite	900	3	$\theta > \delta$	86
e	Boehmite	600	3	γ	40
f	Boehmite	900	3	δ	27

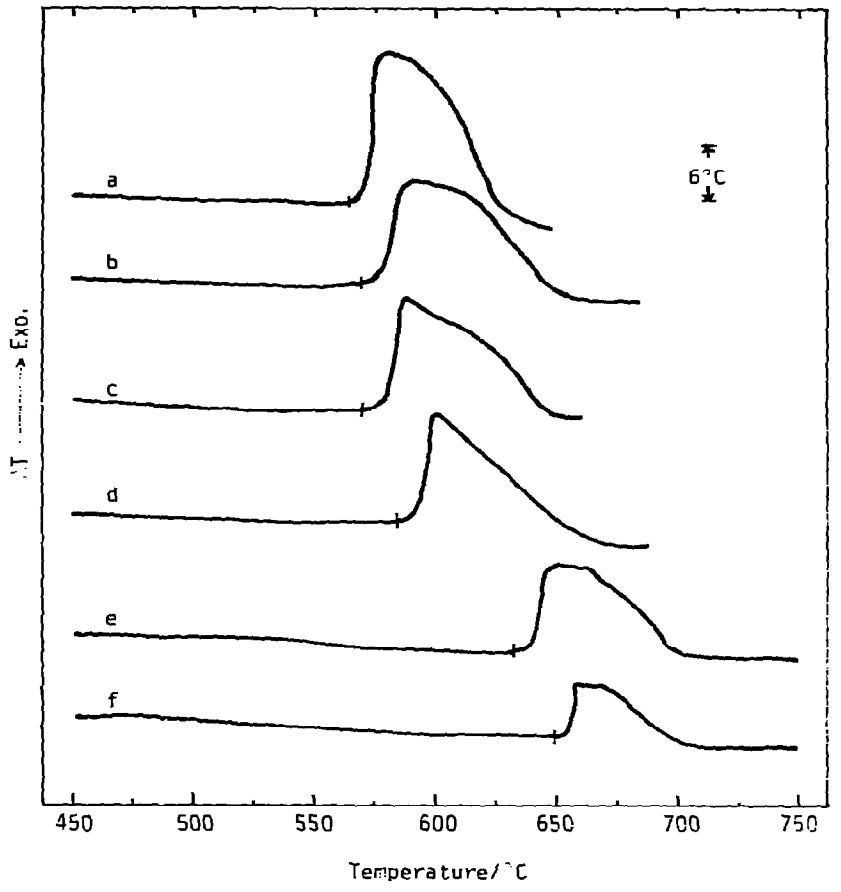

Fig. 3. DTA curves of transition alumina—active carbon (C) systems (wt. ratio 2 : 1) in chlorine. Flow rate of Cl_2, 30 ml min^{-1}; heating rate, 5°C min^{-1}; total weight of sample, 470—500 mg. Signs of curves, a—f, are identical to specimen numbers shown in Table 2.

Al_2O_3 in curves (e) and (f). On the basis of the data in Table 2, the difference in reactivity seems to relate to structures and specific surface areas of transition aluminas. On the other hand, the difference in reactivity between η-Al_2O_3 and θ-Al_2O_3 [compare T_i values of curve (a) with (b), and (c) with (d), respectively) and between γ-Al_2O_3 and δ-Al_2O_3 [compare that of curve (e) with (f)] is very small despite the large difference in the specific surface area of the alumina samples; samples a, c and e have twice the area of samples b, d and f, respectively. Consequently, these facts indicate that the reactivity of transition aluminas for chlorination depends on the structures rather than their specific surface area. Unfortunately, the exact determination of the crystal structure of η-, γ-, δ- and θ-Al_2O_3 has not been accomplished up till now, because no crystals of sufficient size for single crystal X-ray diffraction are available. In general, however, it is known that the oxygen lattice in the transition aluminas is approximately cubic close-packed and the degree of order of packing depends on the pseudomorphic dehydration mechanisms of the starting materials. For example, the arrangement of oxygen ions in bayerite is h.c.p., and conversion to η-Al_2O_3 having the c.c.p.

spinel structure involves an almost complete breaking down and rebuilding of the oxygen sublattice. In the case of boehmite, oxygen ions are c.c.p., so that less rearrangement is required to form the γ-Al_2O_3 structure. Consequently, η-Al_2O_3 has a strong one-dimensional disorder of the cubic close-packed stacking, while for γ-Al_2O_3 the oxygen sublattice is fairly well ordered [3,8]. On the other hand, although there are some discrepancies among the investigators as to the distribution of aluminum ions, it is known that in η- and θ-Al_2O_3 aluminum ions preferentially occupy tetrahedral positions [9], while in γ- and δ-Al_2O_3 they occupy preferentially octahedral positions [8,10]. In conclusion, it is considered that the reactivity of transition aluminas for chlorination is influenced by the degree of stacking disorder of the oxygen ions and of occupation of the tetrahedral interstices by aluminum ions.

ACKNOWLEDGEMENTS

The authors wish to thank Mr. K. Kudo for carrying out some of the DTA experiments. This research has been partially supported by the Government Science Research Grant of the Ministry of Education, Japan.

REFERENCES

1 T. Ishii, R. Furuichi and Y. Kobayashi, Thermochim. Acta, 9 (1974) 39; T. Ishii, R. Furuichi, Y. Kobayashi and S. Shimada, Bull. Fac. Eng. Hokkaido Univ., 71 (1974) 151.
2 T. Ishii, R. Furuichi and K. Kudo, Netsusokutei, 4 (1977) 100.
3 B.C. Lippens and J.J. Steggerda, in B.G. Linsen (Ed.), Physical and Chemical Aspects of Adsorbents and Catalysts, Academic Press, London, 1970, p. 171.
4 Japanese Industrial Standard, M8361 (1968).
5 J. Kinnunen and B. Wennerstrand, Chemist-Analyst, 46 (1957) 92.
6 R. Tertian and D. Papée, Compt. Rend., 241 (1955) 1575; H.C. Stumpf, A.S. Russel, J.W. Newsome and J.W. Tucker, Ind. Eng. Chem., 42 (1950) 1398; M.K.B. Day and U.J. Hill, J. Phys. Chem., 57 (1953) 946.
7 R. Tertian and D. Papée, J. Chim. Phys., 55 (1958) 341.
8 B.C. Lippens and J.H. De Boer, Acta Crystallogr., 17 (1964) 1312.
9 H. Jagodzinski and H. Saalfeld, Z. Kristallogr., Kristallgeom., Kristallphys., Kristallchem., 110 (1958) 197; H. Saalfeld, Neues Jahrb. Mineral. Abh., 95 (1960) 1; S. Geller, J. Chem. Phys., 33 (1960) 676; H. Pines and W.O. Haag, J. Am. Chem. Soc., 82 (1960) 2471.
10 H. Saalfeld and B.B. Mehrota, Ber. Dtsch. Keram. Ges., 42 (1965) 161.